Journal of Cellular Biochemistry 75:686–697 (1999)

# Alterations of the Actin Polymerization Status as an Apoptotic Morphological Effector in HL-60 Cells

**Jian Yu Rao,**[1]* **Yu Sheng Jin,**[1] **QinLong Zheng,**[2] **Jeanne Cheng,**[1] **Jennifer Tai,**[1] **and George P. Hemstreet III**[2]

[1]Department of Pathology and Laboratory Medicine, University of California at Los Angeles and Jonsson Comprehensive Cancer Center, Los Angeles, California 90024
[2]Department of Urology, University of Oklahoma Health Sciences Center, Oklahoma City, Oklahoma 73190

**Abstract** The alterations of the cytoskeletal actin network have been implicated as a morphological effector in apoptosis. However, studies directly linking actin change to the morphological events in apoptosis are lacking. This study quantitatively examined the effect of actin alteration on the camptothecin (CPT)-induced apoptotic process in HL-60 cells. Actin alteration was induced by two distinctive types of agent: the polymerization-stimulating agent, Jasplakinolide (Jas), and the polymerization-blocking agent, cytochalasin B (CB). The actin polymerization status was measured by two complementary methods: the cell pellet-based DNase I inhibition method, and the individual cell-based quantitative fluorescence image analysis (QFIA) assay. Actin polymerization induced by Jas caused apoptosis directly. By contrast, CB, an actin polymerization-blocking agent, partially inhibited CPT-induced apoptosis. A similar inhibition of the CPT-induced apoptosis response was observed with a more specific actin depolymerization agent, cytochalasin E. The alterations of the actin polymerization status occurred in three sequential steps during the apoptotic process: first polymerization, followed by depolymerization, and finally degradation. However, compared with CPT-induced apoptosis, Jas-induced apoptosis was characterized by pronounced actin polymerization that corresponded morphologically with prominent membrane blebbing, but less apoptotic body formation. Furthermore, DNase I activity, which is normally inhibited by G-actin, was specifically detected in Jas-treated cells. These results show that the regulation of actin polymerization is an important apoptotic morphological effector, whereas the alterations of the actin polymerization status by chemicals have profound effects not only on altering the morphology of apoptotic cells, but on apoptosis induction in HL-60 cells as well. J. Cell. Biochem. 75:686–697, 1999. 

**Key words:** actin; apoptosis morphology; Jasplakinolide

Actin is a highly conserved, major functional and structural cytoskeletal protein among all types of eukaryotic cells [Pollard and Cooper, 1986]. Actin exists in cells as G-actin, the globular or nonpolymerized form, or F-actin, the polymerized filamentous form. The dynamics of actin polymerization are regulated by complex intracellular signal transduction events, including calcium/magnesium homeostasis [Pollard and Cooper, 1986], *Src* oncogene [Davis et al., 1991], and members of the *Ras* superfamily, *Rac* and *Rho* [Olson et al., 1995; Nobes and Hall, 1995]. The alterations of the actin network have been implicated in growth control, transformation, and metastasis of tumor cells [Hunter, 1997]. Several actin binding proteins, including vinculin [Fernandez et al., 1992], gelsolin [Tanaka et al., 1995], and tropomyosin [Prasad et al., 1993], exert tumor suppression function. Recently, several studies have confirmed that the alterations of actin polymerization homeostasis per se by certain natural cytotoxins, such as Jasplakinolide (Jas) [Senderowicz et al., 1995; Duncan et al., 1996] and Sphinxolides [Zhang et al., 1997], have profound antiproliferative effects on a number of cancer cell lines.

In addition to the role in proliferation control, actin has also been implicated as a morphologi-

Abbreviations used: ICE, interleukin 1β-converting enzyme; CB, cytochalasin B; Jas, Jasplakinolide; CPT, camptothecin; QFIA, quantitative fluorescence image analysis; FITC, fluorescein.

Grant sponsor: National Cancer Institute–National Institutes of Health; Grant number: R29-CA-71081; Grant number: VA #111-34-0132.

*Correspondence to: Jian Yu Rao, Department of Pathology and Laboratory Medicine, and Jonsson Comprehensive Cancer Center, 13-186 CHS, University of California at Los Angeles, Los Angeles, CA 90024.

Received 3 February 1999; Accepted 1 June 1999

cal effector during apoptosis [Martin and Green, 1995; Kayalar et al., 1996; Mashima et al., 1995, 1997; Peitsch et al., 1993; Ucker et al., 1992]. Several studies observed that actin [Kayalar et al., 1996; Mashima et al., 1995] or actin-modulating proteins, fodrin [Martin et al., 1995], and gelsolin [Kothakota et al., 1997], are substrates of interleukin-I converting (ICE) enzyme or ICE-like proteases, the mediators of the apoptotic cascade. The cleavage of actin or actin-modulating proteins by ICE or ICE-like protease during the apoptotic process presumably alters the homeostasis of the actin polymerization status [Kayalar et al., 1996; Kothacota et al., 1997]. This may, in turn, induce typical morphological changes seen in apoptotic cells. However, evidence for this hypothesis has mostly been indirect. Although several studies previously attempted to evaluate the alterations of actin polymerization during apoptosis [Endresen et al., 1995; Levee et al., 1996; Cotter et al., 1992], these studies were largely nonquantitative, and the experimental results were confusing. For this reason, direct examination of the relationship between the changes in actin and specific morphological events during apoptosis in a quantitative fashion is important.

In this study, an apoptotic model using HL-60 cells and camptothecin (CPT) was used to evaluate the impact of actin-altering agents on the apoptotic process. Two distinctive actin-altering agents were used: Jas, the actin polymerization-stimulating agent [Bubb et al., 1994], and Cytochalasin B (CB), the polymerization-blocking agent. Because CB is known to inhibit glucose transport in addition to the effect on actin polymerization [Sogin and Hinkle, 1980], the results of CB on apoptosis inhibition were verified by a different actin polymerization agent cytochalasin E (CE). The dynamic alterations of the actin polymerization status during the apoptotic process were examined on cells treated with CPT alone, or with both CPT and Jas. Changes in actin polymerization were quantitatively monitored by two different methods: the traditional biochemical DNase I inhibition assay, and the quantitative fluorescence image analysis (QFIA) technique. QFIA, when combined with the fluorescence in situ TUNEL assay, can measure nonpolymerized actin (G-actin) content in TUNEL-positive versus TUNEL-negative cells separately at different time points. The results of this study substantiate the functional role of actin as a morphological effector in apoptosis. The chemical-induced alterations of actin polymerization have profound effects, not only on the cellular morphology of apoptotic cells, but on apoptosis induction as well.

## MATERIALS AND METHODS

### Materials

CB, CE, CPT, bovine pancreatic DNase I, and rabbit muscle-specific actin were obtained from Sigma Chemical Co. (St. Louis, MO). Jas, BODIPY-FL phallacidin, biotin-conjugated phalloidin, and Oregon-Green-labeled and Texas Red-labeled DNase I were obtained from Molecular Probes (Eugene, OR).

### Cell Lines and Cell Culture

HL-60, a human promyelocytic leukemia line, was grown in RPMI 1640 with glutamine (Gibco-BRL, Grand Island, NY), supplemented with 10% heat-inactivated fetal bovine serum (FBS). All cells were maintained in a 5% $CO_2$ atmosphere at 37°C.

### Drug Treatment

Stock solutions of CB, CE, Jas, and CPT were prepared by dissolving the chemicals in absolute ethanol, methanol, or dimethylsulfoxide (DMSO), at concentrations of 10 mg/ml, 10 μM, 500 μM, and 15 mM, respectively. Even with the highest concentrations of drugs used in this study, the final concentrations of these solvents in medium were $<0.1\%$ (v/v), which had minimum effect on the cells.

Logarithmically growing HL-60 cells were harvested and seeded at an initial density of $2 \times 10^6$ cells in 20 ml of fresh medium in a 75-$cm^2$ tissue culture flask. After an overnight proliferation, HL-60 cells were incubated with various concentrations of Jas, CB, CE, or CPT, either alone or in combination, for various time points (2, 4, 8, 12, 24 h).

### Cell Viability, Morphology, and Apoptosis Examination

The total number of viable cells for each condition was determined by trypan blue exclusion test. Cells at various time points and condi-

tions were harvested by pelleting at 800*g* for 10 min, and then aliquoting into several tubes. One tube of cells was fixed with 1% formaldehyde for 15 min, washed once with phosphate-buffered saline (PBS), followed by 70% ethanol. These cells were kept at −20°C for subsequent TUNEL assay for apoptosis examination, and QFIA for the analysis of G-actin content. The remaining tubes of cells, one for actin quantification by DNase I inhibition assay and one for DNA zymogram analysis, were frozen as pellets at −70°C until analysis.

Microscope slides were prepared using cytospin (Sadon, 500*g*, 10 min) for each experimental condition from fixed cells. Slides were used for slightly modified in situ labeling of DNA breaks, terminal deoxytransferase-mediated BrdUTP Nick End-Labeling, or TUNEL assay. This procedure was carried out at a separate laboratory, in a blinded fashion. TdT and reaction buffer were purchased from Boehringer-Mannheim (Indianapolis, IN). Briefly, cells on cytospin slides were incubated with 50 µl of a solution containing 10 µl of reaction buffer, 2 µl of BrdUTP stock solution, 0.5 µl of TdT in storage buffer, 5 µl of $CaCl_2$ solution, and 32.5 µl of distilled $H_2O$ in a humidified chamber for 60 min at 37°C. Slides were then rinsed by adding 250 µl of rinsing buffer, and then washed twice with PBS. Next, the slides were incubated with 100 µl of fluorescein-conjugated anti-BrdUrd McAb (Becton Dickinson, NY) solution for 1 h at room temperature. Nuclear DNA was also labeled by adding 200 µl of Hoechst 33258 staining solution on the slides and incubating for 5 min at room temperature. For each slide, 300 cells were counted and the percentage of apoptotic cells was calculated using QFIA.

### DNA Isolation and Agarose Gel Electrophoresis

To detect apoptotic DNA fragments, a modification of the method of Herrmann et al. [1994] was used. Cultured cells were washed with PBS and pelleted by centrifugation at 1,500 rpm for 5 min. Cells were then resuspended in Nonidet-40 (NP-40) lysis buffer (1% NP-40 in 20 mM EDTA, 50 mM Tris-HCl, pH 7.5) for 10–20 s. After centrifugation at 2,000*g* for 5 min, the supernatant was transferred into a new tube, and the extraction procedure was repeated once with the same amount of lysis buffer. The supernatant was collected after adding 0.5 vol 10 M ammonium acetate and 2.5 vol 100% ethanol and freezing at −80°C for 30 min. After centrifugation at 10,000 rpm for 15 min, DNA fragments were washed with 70% ethanol and dried at room temperature. The DNA pellet was dissolved with TE Buffer, pH 8.0, and loaded on a 1% agarose gel containing ethidium bromide (0.4 µg/ml).

### Quantitative Fluorescence Image Analysis (QFIA)—TUNEL/G-Actin/DNA Triple Label Assay to Measure the G-Actin Level on Individual Cell Basis

To monitor accurately the actin polymerization status in cells undergoing apoptosis, a triple fluorescence labeling procedure was carried out. To do so, cells on slides were first labeled with fluorescein isothiocyanate (FITC)-conjugated TUNEL labeling for apoptosis and Hoechst 33258 for DNA, as described above. Cells were further incubated with a G-actin labeling reagent, Texas Red-conjugated DNase I (1:500 v/v), for 30 min. The QFIA analysis of G-actin with minor modifications can be found elsewhere [Rao et al., 1997]. In brief, the fluorescence intensity of G-actin (Texas Red) and 3′ end DNA breaks (FITC) was quantified simultaneously using the IBAS image analysis system (Roche Image Analysis Systems, Elon College, NC), configured with a Zeiss Axiotron (NY) fluorescent microscope, a motorized computer controlled 8-slide stage, and autofocus. Only intact cells were selected for measurement. These cells were identified, randomly based on nuclear staining of DNA with Hoechst (excitation at 360 ± 50 nm, 400 nm DCLP, and 480 ± 50-nm emission filter), regardless of other fluorescence (FITC and Texas Red). Cell debris and separated apoptotic bodies were excluded from the analysis. Images of the same cells at computer-controlled excitations of 485 ± 22 nm for FITC-labeled apoptosis (505 DRLP, 530 ± 30-nm emission filter) and 560 ± 40 nm for Texas Red-labeled G-actin (595 nm DRLP, 630 ± 23-nm emission filter) were captured using a SIT camera (Hamamatsu, NJ). Specific measurements, including the average gray value of all pixels (fluorescence intensity) within the cells and the area (cell size), were calibrated inmicrons. Approximately 300–500 cells were measured on each slide. Corresponding values of G-actin, DNA, and 3′ end apoptosis labeling for each cell were automatically stored in the database. Generally, the average of the gray mean of G-actin (AGM) was calculated to reflect the G-actin level of that slide, regardless of

apoptotic labeling. The value of AGM was converted to absolute quantitative value (μg/$10^6$ cells), using exactly the same method as previously described [Rao et al., 1997]. If indicated, the population of apoptotic cells was separated from that of nonapoptotic cells based on the cutoff gray mean level that was set by the gray mean level of known apoptotic cells (HL-60 treated with CPT for 8 h).

### DNase I Inhibition Assay for Actin Quantification

The previously described DNase I inhibition method was used without modification for G-actin and total actin quantification [Blikstad et al., 1978; Rao et al., 1997]. The quantity of F-actin was derived by subtracting that of G-actin from total actin, and thereby the ratio of F-actin to G-actin was determined.

### DNA Zymogram for DNase I Activity

A modified DNA zymogram technique based on the technique described by Rauch et al. [1997] was employed to detect DNase I activity. Briefly, cells were cultured, collected, and washed according to the methods described above. Protein extracts were prepared by incubating cell pellets with 5 vol of ice-cold 10 mM Tris, pH 7.6, containing PMSF (0.3 mg/ml) at room temperature for 30 s and centrifuged at 14,000 rpm, 4°C for 30 min. The resulting protein samples were subjected to standard DNA zymogram on a sodium dodecyl sulfate (SDS) gel saturated with 10 μg/ml salmon sperm DNA. Bovine pancreatic DNase I (Sigma Chemical Co., St. Louis, MO) at 0.01 kunitz was used as control. After electrophoresis, the gel was washed four times for 30 min with 200 ml, 40 mM Tris-HCl, pH 7.6, to remove SDS and induce renaturation of the enzyme. The gel was then incubated at room temperature with 200 ml, 40 mM Tris-HCl, pH 7.6, containing 10 mM $MgCl_2$ and 2 mM $CaCl_2$ for 16–24 h to activate the enzyme. Then the gel was stained with ethidium bromide. The presence of a blank band indicated enzymatic activity.

## RESULTS

### Effects of Actin-Altering Agents on Apoptosis Induction of HL-60 Cells

To determine the impact of actin alterations on apoptosis, the effects of various actin-altering agents on apoptosis induction in HL-60 cells were tested. Two kinds of actin-altering agents were studied: CB, the polymerization-blocking agent, and Jas, the polymerization-stimulating agent. Cells were treated either with these agents alone or together with CPT. The actin polymerization-stimulating agent, Jas, at 100 nM concentration, induced immediate apoptosis in HL-60 cells. As detected by TUNEL assay, 50% of the cells underwent apoptosis after a 4-h incubation, and at 12 h, more than 90% cells were TUNEL positive (Fig. 1a). The effect of Jas (100 nM) on apoptosis induction was similar to that of CPT at a concentration of 150 nM. A synergistic effect was not observed between Jas and CPT because cells that were treated with Jas and CPT together for 4 h did not show a further increase in the percentage of TUNEL positive cells (Fig. 1a). To confirm that Jas-induced cell death was indeed apoptosis, DNA agarose gel electrophoresis assay was carried out. DNA ladder formation, the hallmark of apoptotic cells, was detectable at about the same time (Fig. 1b, lanes 5–7) as CPT-induced apoptosis (Fig. 1b, lanes 8–9), indicating the cell death induced by Jas was an apoptotic process. The actin polymerization-blocking agent, CB, had no effect on HL-60 cells when treated alone at 5 μg/ml. By contrast, CB partially inhibited apoptosis when co-incubated with CPT. Compared with CPT-incubated cells, the percentage of apoptosis in CB and CPT co-incubated cells decreased at each corresponding time point (Fig. 1a) while DNA ladder formation at both 4 h and 8 h was less prominent (Fig. 1b, 7 cf. lanes 10 and 11 with lanes 8 and 9). These results suggest that the alterations of actin may have profound effects on apoptosis induction because blocking actin polymerization inhibits apoptosis, whereas stimulating actin polymerization induces apoptosis directly.

To perform a more critical test that CB-induced apoptosis inhibition is mediated by actin alteration, rather than by inhibition of the glucose transporter, the above experiment was repeated using a different agent, CE. Initial experiments using three different concentrations of CE (0.05, 0.5, and 5 μg/ml) showed that a maximum inhibition of apoptosis was observed at the concentration of 0.5 μg/ml (data not shown). As shown in Figure 1c, CE itself did not induce apoptosis but had a profound inhibi-

tory effect on CPT-induced apoptosis. As shown for CB, the percentage of apoptosis in cells co-incubated with CE and CPT was substantially lower than that in cells treated with CPT alone (Fig. 1c) at all time points.

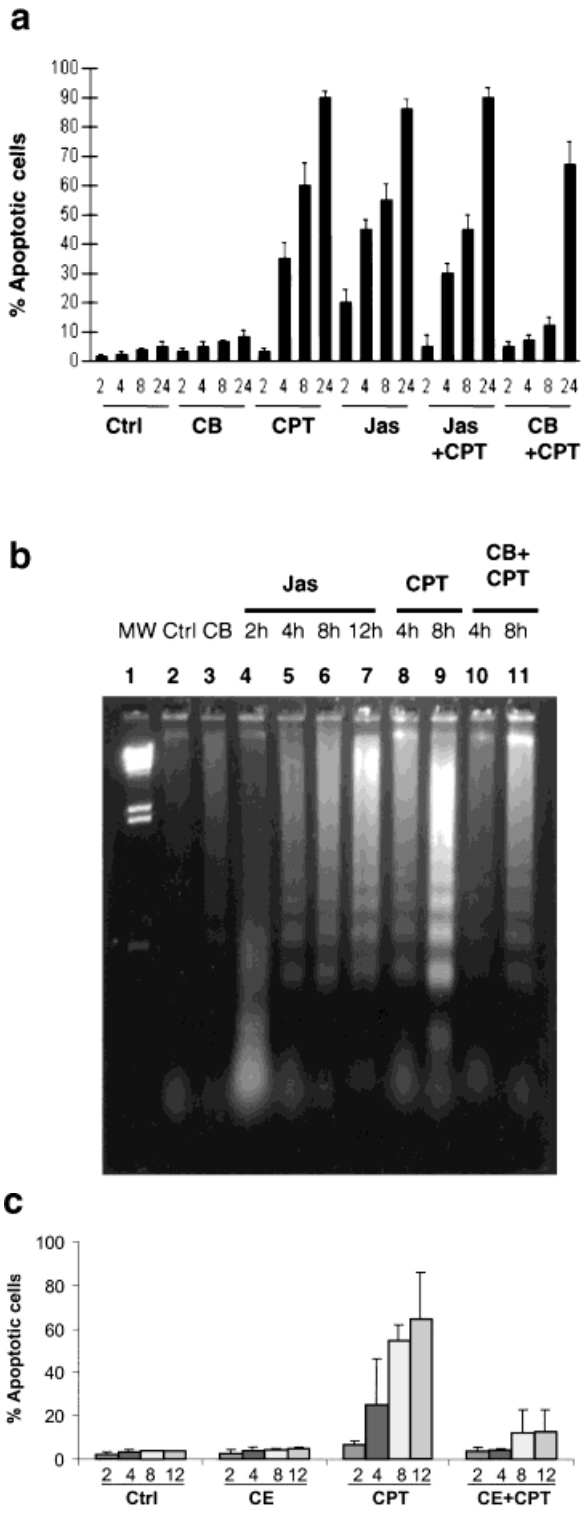


## Alterations of Actin Polymerization During CPT-Induced Apoptosis in HL-60 Cells

To characterize how the actin polymerization status might be altered during the apoptotic process, both G- and F-actin levels were quantitatively monitored simultaneously using two different methods: the DNase I inhibition assay and the QFIA method. The number of apoptotic cells in CPT-treated (0.15 μM) HL-60 cells increased gradually with time and, by 24 h, more than 90% cells underwent apoptosis (Fig. 1a). Figure 2a shows the changes of the actin polymerization status measured by DNase I inhibition assay at different time points during the CPT-induced apoptotic process in HL-60 cells. There was transient actin polymerization at 0–2 h after CPT treatment. The F/G-actin ratio, an indicator for the actin polymerization status, increased from the baseline level of 1.27–2.22. However, at 2–4 h, actin became depolymerized, whereas the F/G-actin ratio at 4 h decreased to 1.03. Thereafter, actin was degraded with the total actin content (the sum of G- and F-actin) decreased gradually.

Because the DNase method is a cell pellet-based assay, the actin level measured by this method may be confounded by the variation of the number of dead cells at different time points. To pinpoint accurately the stage in which actin depolymerization occurs, the QFIA DNA/G-actin/TUNEL triple-label assay was employed to measure the G-actin levels in TUNEL-positive and TUNEL-negative cells separately at different time points. Because the results of both Northern blot analysis and Western blot analysis did not show changes in either β-actin gene expression or net actin synthesis (data not shown), increased G-actin content above the baseline level (at 0 time point) indicates actin depolymerization. Conversely, a decreased G-actin content below the baseline level indicates actin polymerization. As shown in Figure 2b,

**Fig. 1.** Effect of Jas, CB, CE, and CPT on apoptosis induction in HL-60 cells. **a:** Percentage of apoptosis determined by in situ end-labeling (TUNEL) assay in cells treated with solvent control (EtOH/DMSO), Jas (100 nM), CB (5 μg/ml), CPT (150 nM), Jas + CPT, and CB + CPT at different time points. The length of the vertical bar represents 1 SD of three independent experiments. **b:** Representative results of DNA agarose gel electrophoresis in HL-60 cells. **c:** Percentage of apoptosis as in **a** in cells treated with solvent control (DMSO), CE (0.5 μg/ml), CPT (150 nM), and CE + CPT at different time points.

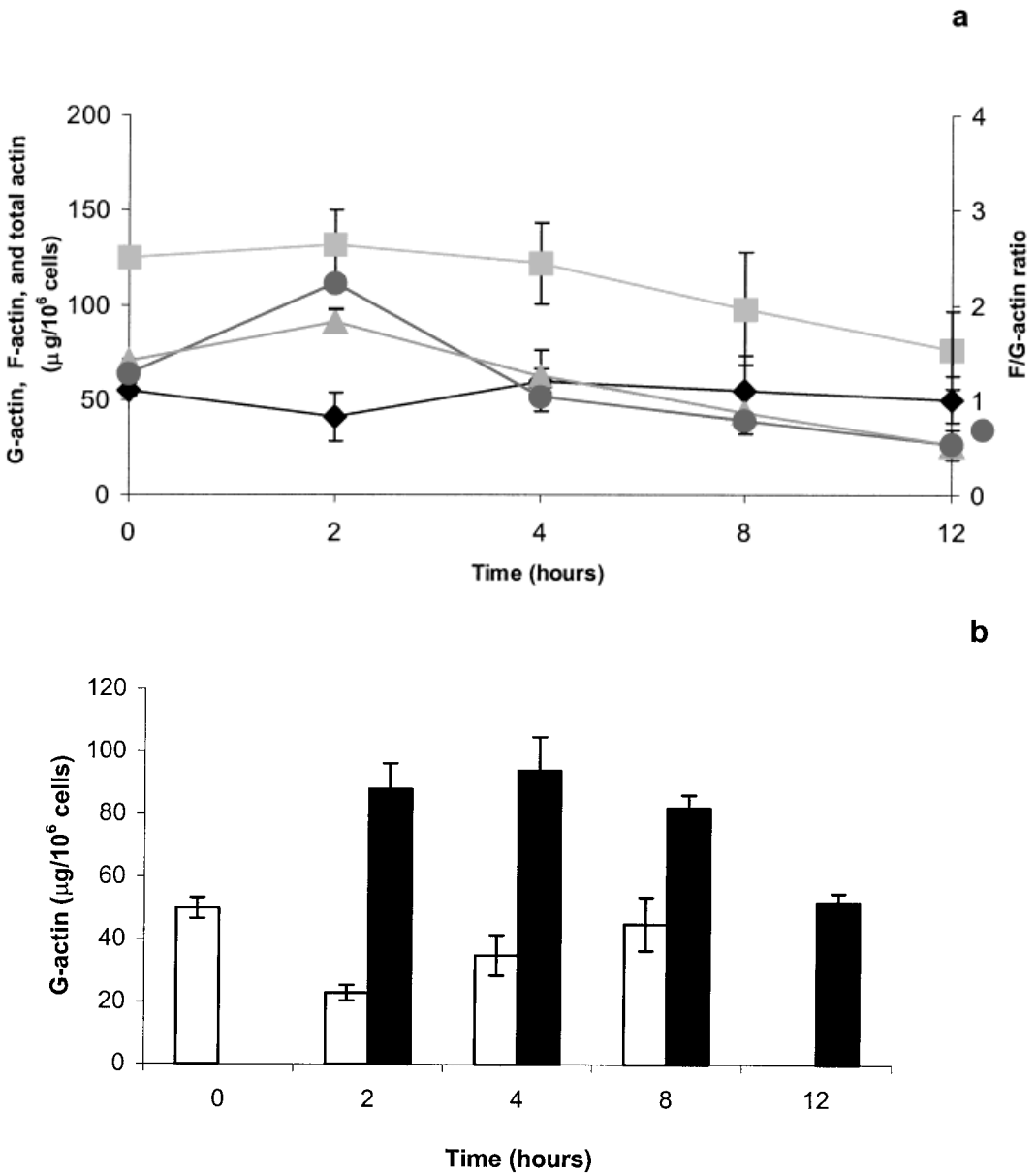


**Fig. 2.** Dynamic changes of the actin polymerization status during the CPT induced apoptotic process in HL-60 cells. **a:** Results of DNase I inhibition assay (mean ± SD based on three independent experiments). ■, total actin; ●, F-/G-actin ratio; ◆, G-actin; ▲, F-actin. **b:** Results of QFIA analysis for the G-actin level (μg/$10^6$ cells) in TUNEL-positive versus -negative cells (mean ± SD based on three independent experiments, approximately 300–500 cells were measured for each experiment) at different time points. Blank columns represent TUNEL-negative cells; solid columns represent TUNEL-positive cells.

G-actin of TUNEL-negative cells showed a transient decrease below the baseline level at 2 h, suggesting that actin was polymerized at an early stage of the apoptotic process. In TUNEL-positive cells, G-actin increased to above the baseline level during the 2- to 8-h period, indicating that actin was depolymerized in apoptotic cells during this period. Because TUNEL labeling in a cell signifies DNA double-strand breakage, we conclude that actin depolymerization occurred after DNA breakage. However, the G-actin level in TUNEL positive cells decreased thereafter, reaching the baseline level at 12 h. This observation is consistent with the above finding that actin is degraded at the later phase of cell death. Together these results suggest that during the CPT-induced cell death process, actin follows a three-step change that

begins with a transient polymerization, followed by depolymerization, and finally degradation.

### Alterations of the Actin Polymerization Status During the Jas-Induced Apoptotic Process

Changes of the actin polymerization status during the Jas-induced apoptotic process in HL-60 cells were measured using the same method described above. The results are presented in Figure 3a,b. Similar to CPT-induced apoptosis, actin was initially polymerized and then depolymerized (Fig. 3a). However, actin polymerization of Jas-treated cells was more pronounced compared with that of CPT-treated cells (cf. Figs. 3a and 2a). The F/G-actin ratio increased from 1.38 at baseline level (0 h) to 3.26 at 4 h and then decreased gradually to 1.75 at 8 h and 0.77 at 12 h. Total actin did not decrease as in CPT-treated cells. These findings are not surprising because of the constitutive effect of Jas on actin polymerization. QFIA analysis showed that G-actin levels in TUNEL-positive cells increased gradually with time (Fig. 3b) and were above the baseline level (0 time point) after 4 h, indicating that even in TUNEL-positive cells, actin depolymerization did not occur until after a 4-h incubation. As expected, TUNEL-negative cells showed a persistent low G-actin level in Jas-treated cells, owing to the constitutive actin polymerization effect of Jas on HL-60 cells.

### Correlation of Actin Changes With the Morphological Events in CPT, Jas, and CB + CPT-Treated Cells

Figure 4 shows representative phase-contrast images (a,c,e,g) and fluorescence images (b,d,f,h) of FITC-TUNEL-labeled cells under different treatment conditions and at different time periods. The phase-contrast image of cells was used because it best revealed membrane bleb formation at an early stage of incubation (2 h), while the fluorescence image was employed to show apoptotic body formation at later stage of incubation (8 h). At an early stage of incubation (2 h), compared with untreated controls (Fig. 4a), HL-60 cells treated with CPT showed shrinkage of cells with wrinkled cellular outline and scattered, although less prominent, membrane bleb formation (Fig. 4c). By contrast, Jas-treated cells showed much more prominent membrane surface bleb formation (Fig. 4e, indicated by closed arrows). Cells co-incubated with CPT and the actin polymerization-blocking agent, CB (Fig. 4g), showed similar morphological changes to those of cells treated with CPT alone (Fig. 4c). At later stage (8 h), however, cells that were treated with CPT alone (Fig. 4d) showed more prominent apoptotic body formation (indicated by an open arrow) than cells that were treated with Jas (Fig. 4f). Cells co-incubated with CPT and CB showed a reduced number of apoptotic cells, as well as less prominent apoptotic body formation (Fig. 4h), compared with cells treated with CPT alone.

The findings described above suggest that actin polymerization is related to membrane bleb formation and that the subsequent depolymerization is associated with apoptotic body formation. This is consistent with the observations reported by Levee et al. [1996]. Furthermore, the observation that actin polymerization-stimulating agent induced more prominent membrane blebbing but less apoptotic body formation, whereas actin polymerization-blocking agent inhibited the entire apoptotic process, indicates that early actin polymerization is an essential step for the subsequent series of morphological events. Actin polymerization results directly in membrane blebbing, whereas the subsequent depolymerization that occurs after DNA fragmentation may predispose to apoptotic body formation.

### Detection of DNase I Activity During the Apoptotic Process in HL-60 Cells

G-actin is a natural inhibitor of DNase I, an enzyme thought by some to be a possible endonuclease that causes DNA fragmentation in apoptotic cells [Peitsch et al., 1993; Ucker et al., 1992]. To determine whether Jas-induced DNA fragmentation is mediated by DNase I, the DNase I activity was evaluated during the Jas- and CPT-induced apoptotic process using a modified DNA zymogram technique. As shown in Figure 5, the enzyme activity, represented by a black band at the same site as the DNase I standard control in a sodium dodecyl sulfate-polyacrylamide gel electrophoresis (SDS-PAGE) gel saturated with DNA, was detectable after 4 h of Jas treatment and was highest at 12 h. The enzyme requires $Ca^{2+}$ and $Mg^{2+}$ for activation and most of all, the enzyme activity can be completely inhibited by adding actin into the

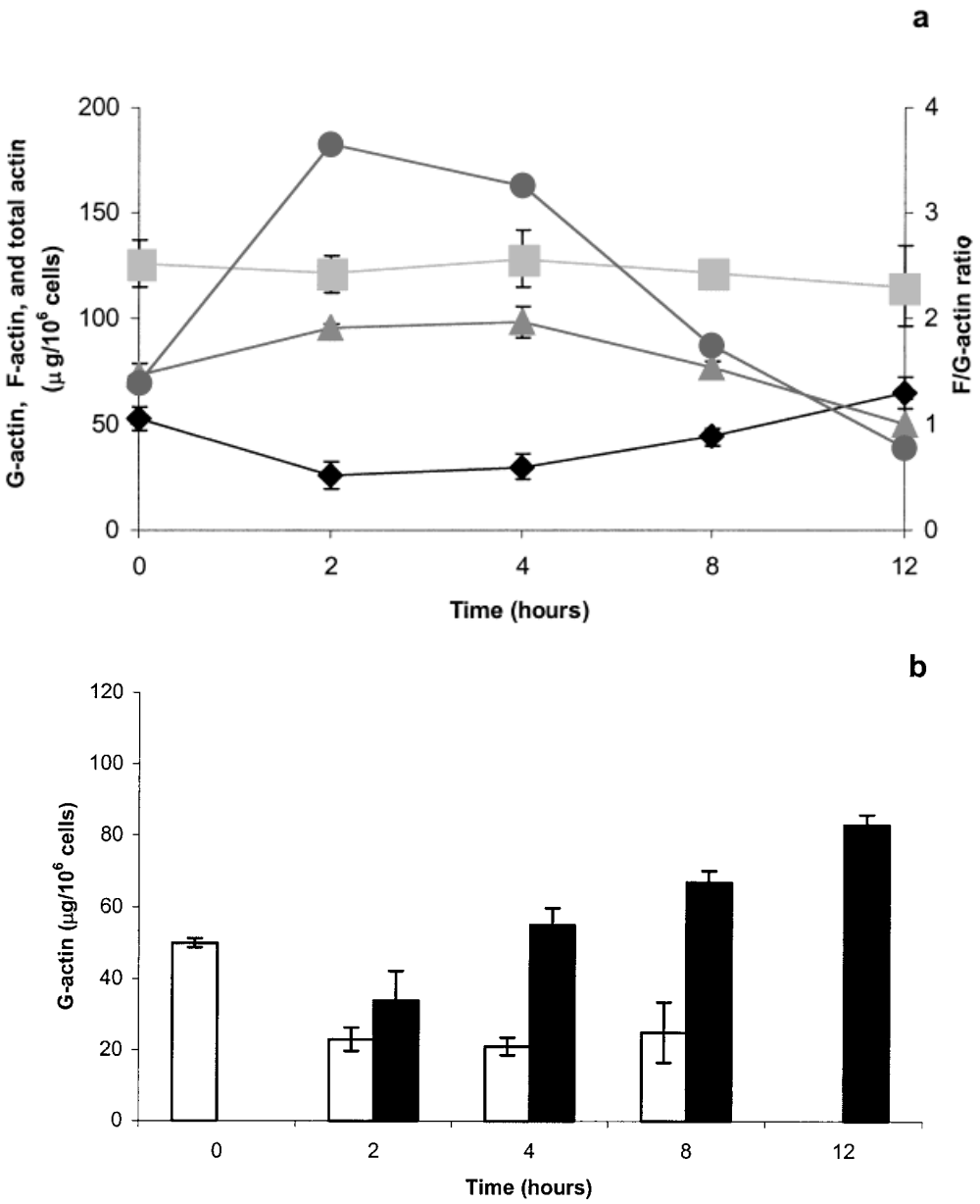


**Fig. 3.** Dynamic changes of the actin polymerization status during the Jas-induced apoptotic process in HL-60 cells. **a:** Results of DNase I inhibition assay (mean ± SD based on three independent experiments). ■, total actin; ● , F-/G-actin ratio; ◆, G-actin; ▲, F-actin. **b:** Results of QFIA analysis for the G-actin level (μg/$10^6$ cells) in TUNEL-positive versus negative cells (mean ± SD based on three independent experiments, approximately 300–500 cells were measured for each experiment). Blank columns represent TUNEL negative cells and solid columns represent TUNEL-positive cells.

activation incubation buffer (not shown). These results confirm that this enzyme was DNase I. DNase I activity correlates with the decline of G-actin (Fig. 3a,b) on one hand, and the emerging of DNA fragmentation on the other (Fig. 1b). This DNase I activity was not detected in CPT-treated HL-60 cells, suggesting that another endonuclease may be involved in CPT-induced apoptosis.

## DISCUSSION

The cytoskeleton of eukaryotic cells consists of an extensive network of microfilaments, intermediate filaments, and microtubules. Disruption of these networks results in many fundamental changes of cellular structure and function, including morphological alteration, dissociation of mitosis, and cell death [Pollard

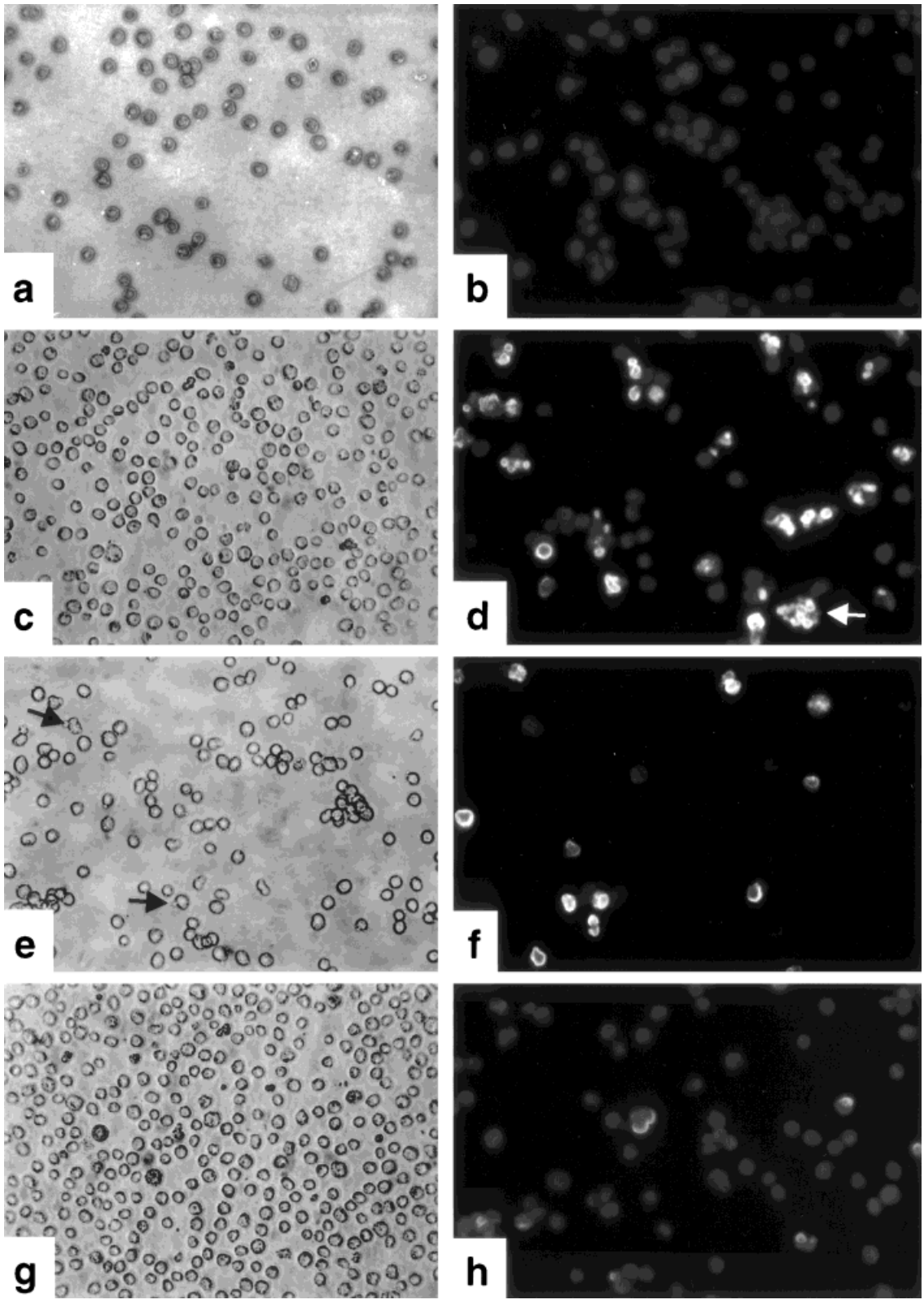


**Fig. 4.** Effects of CPT, Jas, and CB + CPT on the morphology of HL-60 cells. Phase-contrast images (a, c, e, g) were taken at 2 h after incubation. Fluorescence images (b, d, f, h) were taken at 8 h after incubation while the cells were labeled with FITC-TUNEL for apoptotic cells. **a,b:** Nontreated control. **c,d:** CPT (150 nM). **e,f:** Jas (100 nM). **g,h:** CB (15 μg/ml) + CPT (150 nM). All images were taken with an original magnification at ×63. Closed arrows (**e**) indicate membrane bleb formation, while the open arrow (**d**) shows apoptotic body formation.

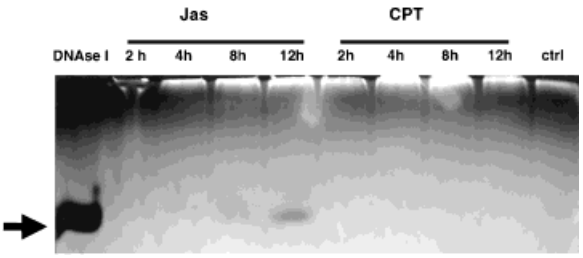


**Fig. 5.** Detection of DNase I activity in HL-60 cells treated with Jas and CPT. Cells at different conditions were collected to prepare protein lysates as described under Materials and Methods. These protein extracts were run on a SDS-PAGE gel saturated with salmon sperm DNA. The gel was renatured and the enzyme activated by incubation with solutions containing appropriate concentrations of cations. DNase I activity was indicated by the presence of a blank band in the gel, at the position corresponding to the pure bovine pancreatic DNase I (0.01 kunitz unit).

and Cooper, 1986]. Chemicals directed against microtubules have been used clinically as antitumor chemotherapeutic agents. Actin-disrupting agents have also recently emerged as potential new classes of chemopreventive agents. For instance, Jas [Senderowicz et al., 1995] and Sphinxolides [Zhang et al., 1997] are two chemotherapeutic agents that function at the microfilament level to inhibit the proliferation of cell lines, including tumor cells with multiple drug resistance [Zhang et al., 1997].

The apoptotic process in the cell culture system usually presents with sequential morphological changes—cytoplasmic membrane blebbing, followed by internucleosomal DNA fragmentation, and finally, apoptotic body formation [Cotter and Al-Rubeai, 1995]. The fact that these features are common, but may vary to a certain degree, during the apoptotic process in various cell types suggests that some highly conserved but complex biochemical systems may be involved. One such system is the network of cytoskeletal actin and/or actin-related proteins [Martin and Green, 1995]. Although recent studies indicate that actin may be responsible for the typical morphological changes of apoptotic cells, direct quantitative studies correlating the changes in actin with the morphological events of the apoptotic process are lacking. In this study, it was observed that actin was initially polymerized and later depolymerized and eventually degraded during CPT-induced apoptosis in HL-60 cells. Early polymerization is a crucial event because alterations in the polymerization status by Jas, CB, and CE have profound effects on the morphology and induction of apoptosis in HL-60 cells.

CB has two modes of function: binding F-actin to block polymerization, and inhibition of glucose transporter [Sogin and Hinkle, 1980]. This study showed that CE, a more specific actin polymerization-inhibiting agent demonstrates an inhibitory effect on apoptosis induction similar to that observed with CB. This observation suggests that CB-induced apoptosis inhibition is more likely mediated by actin polymerization-blocking function, rather than through inhibition of the glucose transporter.

While actin polymerization-blocking agents (CB and CE) inhibited CPT-induced apoptosis in HL-60 cells, the actin polymerization-stimulating agent, Jas, directly induced immediate apoptosis. It was also observed that Jas potentiated CPT-induced apoptosis in K562 cells (data presented in a separate paper). K562 is a chronic myelocytic leukemic cell line that is usually resistant to chemicals such as CPT [Cotter and Al-Rubeai, 1995]. These findings together argue that the alterations of actin during apoptosis are active phenomena, rather than passive degradation effects of cell death.

Figure 6 summarizes the morphological features and the corresponding changes in the actin polymerization status during different phases of the CPT- and Jas-induced apoptotic process. Compared with CPT-induced apoptosis, Jas-induced apoptosis prolonged actin polymerization in HL-60 cells, while the concomitant apoptotic process was characterized by earlier and prominent membrane bleb formation, but delayed apoptotic body formation. Consistent with the results from others [Endresen et al., 1995; Levee et al., 1996; Cotter et al., 1992], the actin polymerization-blocking agent, CB, inhibited both membrane blebbing and apoptotic body formation. These findings suggest that the apoptotic morphological events be regulated by the actin polymerization status. Actin polymerization leads to membrane surface blebbing, whereas subsequent depolmerization relates to apoptotic body formation. However, these two phenomena are interdependent, rather than isolated events, because CB, the actin polymerization-blocking agent, inhibits not only membrane bleb formation, but also apoptotic body formation.

The current observation that Jas-induced apoptosis in HL-60 cells was coupled to a detectable increased DNase I activity is intriguing.

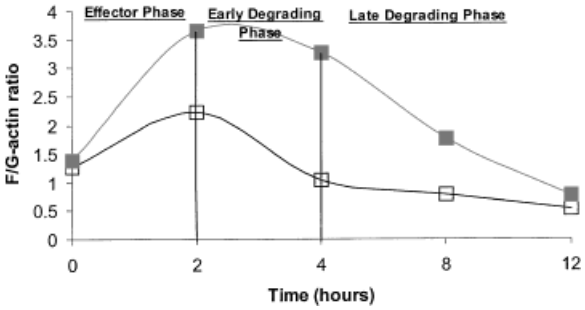


**Fig. 6.** Correlation of the morphological events with actin change during different periods of the CPT (□) and the Jas (■)-induced apoptotic processes in HL-60 cells. There are three phases: effector phase, early degrading phases, and late degrading phases. During the effector phase, actin is polymerized that correlates with membrane bleb formation in both the CPT- and the Jas-induced apoptotic processes. However, both actin polymerization and membrane bleb formation are more pronounced in Jas-treated cells. In early degrading phase, actin depolymerization occurs in CPT-induced apoptotic process that correlates with early apoptotic body formation. In Jas-induced apoptotic process, actin remains polymerized while DNA fragmentation begins to appear. During the late degradation phase, actin is degraded in the CPT-induced apoptotic process, while in the Jas-induced apoptotic process, actin depolymerization begins to occur.

Although other potential mechanisms may explain the observed effect of Jas on apoptosis induction, our findings provide direct evidence to support the argument that a novel mechanism involving actin alteration and apoptosis induction may exist. G-actin is a natural inhibitor of DNase I, the enzyme thought by some as the potential endonuclease causing typical DNA fragmentation seen in apoptosis [Ucker et al., 1992]. This hypothesis has been debated intensively and has still not been resolved, partly because no changes of DNase I activity have been detected in cells undergoing apoptosis. The recent cloning of Caspase-activated DNase (CAD) [Enari et al., 1998] is a breakthrough in identifying the endonuclease in the apoptotic process. However, the finding of CAD does not rule out the possibility that under certain conditions, other enzymes such as DNase I may be involved. In fact, our observation that actin overpolymerization induced DNase I activation and immediate apoptosis, whereas blocking actin polymerization by CB inhibited CPT induced apoptosis, suggests that at least in HL-60 cells, the G-actin–DNase I interaction is a novel mechanism of apoptosis induction. The finding reported by Kayalar et al. [1996] that ICE-cleaved-actin cannot inhibit DNase I in vitro and reported by Madaio et al. [1996] that DNA/DNase I autoantibodies modulate nuclear apoptosis in living cells also supports this model. However, changes of DNase I activity were not detected in CPT-treated cells, suggesting that another endonuclease, such as CAD, may be involved. It should be noted that other studies did not observe an inhibitory effect of CB on DNA fragmentation, while in the current study, a clear inhibitory effect of CB on CPT-induced DNA fragmentation was observed [Levee et al., 1996]. This difference may be attributable to the fact that different model systems were used. Actin alterations have also been observed in other cell models such as ultraviolet (UV)-induced apoptosis [Levee et al., 1996], p53-mediated apoptosis in HL-60 cells [Guenal et al., 1997], or spontaneous cell death in neutrophils [Brown et al., 1997]. Although the alterations of actin may be present in different forms, the fact that actin change is seen in different model systems strongly supports the notion that actin alteration may be a common effector event in the process of apoptosis.

In summary, this study confirms that the alterations of actin involve all three major morphological changes associated with the apoptotic process: membrane blebbing, DNA fragmentation, and apoptotic body formation. These findings provide evidence for the hypothesis that cytoskeletal actin alteration is potentially one of the final morphological effectors in the mechanism of cell death [Martin and Green, 1995]. The results do not imply that actin change is the sole effector for all apoptotic events. Other potentially important effectors, such as CAD, DNA-PK, or other cytoskeletal proteins, may also be involved. Nevertheless, the fact that the alterations of the actin polymerization status not only change the phenotypic appearance of apoptosis, but also influence the susceptibility of cells to apoptosis stimulators, may provide a new avenue for circumventing tumor drug resistance. These in vitro observations indicate a potential signaling pathway that may be operative in vivo. Studying the effects of these agents on premalignant lesions within the context of their microecosystems may eliminate the problems of genetic instability and enhance therapeutic success.

## ACKNOWLEDGMENTS

The authors thank Linda Baum, Patricia Ganz, Sanford Barsky, and Charles Sawyers for

reading the manuscript and providing valuable discussions.

## REFERENCES

Blikstad I, Markey F, Carlsson L, Persson T, Lindberg U. 1978. Selective assay of monomeric and filamentous actin in cell extracts, using inhibition of deoxyribonuclease I. Cell 15:935–943.

Brown SB, Bailey K, Savill J. 1997. Actin is cleaved during constitutive apoptosis. Biochem J 323(pt 1):233–237.

Bubb M, Senderowicz A, Sausville E, Duncan K, Korn E. 1994. Jas, a cytotoxic natural product, induces actin polymerization and competitively inhibits the binding of phalloidin to F-actin. J Biol Chem 269:14869–14871.

Cotter T, Al-Rubeai M. 1995. Cell death (apoptosis) in cell culture systems. Trends Biotechnol 13:150–155.

Cotter T, Lennon S, Glynn J, Green D. 1992. Microfilament-disrupting agents prevent the formation apoptotic bodies in tumor cells undergoing apoptosis. Cancer Res 52:997–1005.

Davis S, Lu M, Lo S, Lin S, et al. 1991. Presence of an SH2 domain in the actin-binding protein tensin. Science 252: 712–715.

Duncan M, Harmon J, Duncan K. 1996. Actin disruption inhibits bombesin stimulation of focal adhesion kinase (pp125FAK) in prostate carcinoma. J Surg Res 63:359–363.

Enari M, Sakahira H, Yokkoyama H, Okawa K, Iwamatsu A, Nagata S. 1998. A caspase-activated DNase that degrades DNA during apoptosis, and its inhibitor ICAD. Nature 391:43–50.

Endresen P, Fandrem J, Eide T, Aarbakke J. 1995. Morphological modifications of apoptosis in HL-60 cells: effects of homocysteine and cytochalasins on apoptosis initiated by 3-deazaadenosine. Virchows Arch 426:257–266.

Fernandez J, Geiger B, Salomon D, Sabanay I, Zoller M, Ze'ev A. 1992. Suppression of tumorigenicity in transformed cells after transfection with Vinculin cDNA. J Cell Biol 119:427–438.

Guenal I, Risler Y, Mignotte, B. 1997. Down-regulation of actin genes precedes microfilament network disruption and actin cleavage during p53-mediated apoptosis. J Cell Sci 110(pt 4):489–495.

Herrmann M, Lorenz H, Voll R, Grunke M, Woith W, Kalden J. 1994. A rapid and simple method for the isolation of apoptotic DNA fragments. Nucleic Acids Res 22:506–507.

Hunter T. 1997. Oncoprotein networks. Cells 88:333–346.

Kayalar C, Ord T, Testa M, Zhong L, Bredesen D. 1996. Cleavage of actin by interleukin 1β-converting enzyme to reverse DNase I inhibition. Proc Natl Acad Sci USA 93:2234–2238.

Kothakota S, Azuma T, Reinhard, et al. 1997. Caspase-3-generated fragment of gelsolin: effector of morphological change in apoptosis. Science 278:294–298.

Levee M, Dabrowska M, Lelli J, Hinshaw D. 1996. Actin polymerization and depolymerization during apoptosis in HL-60 cells. Am J Physiol 271:C1981–1992.

Madaio M, Fabbi M, Tiso M, Daga A, Puccetti A. 1996. Spontaneously produced anti-DNA/DNase I autoantibodies modulate nuclear apoptosis in living cells. Eur J Immunol 26:3035–3041.

Martin S, Green D. 1995. Protease activation during apoptosis: death by a thousand cuts. Cell 82:349–352.

Martin S, O'Brien G, Nishioka W, et al. 1995. Proteolysis of fodrin (non-erythroid spectrin) during apoptosis. J Biol Chem 270:6425.

Mashima T, Naito M, Fujita N, Noguchi K, Tsuruo T. 1995. Identification of actin as a substrate of ICE and ICE-like protease and involvement of an ICE-like protease but not ICE in VP-16-induced U937 apoptosis. Biochem Biophys Res Commun 217:1185–1192.

Mashima T, Naito M, Noguchi K, Miller D, Nicholson D, Tsuruo T. 1997. Actin cleveage by CPP-32/apopain during the development of apoptosis. Oncogene 14:1007–1012.

Nobes C, Hall A. 1995. Rho, Rac, and Cdc42 GTPases regulates the assembly of multimolecular focal complexes associated with actin stress fibers, lamellipodia, and filopodia. Cell 81:53–62.

Olson M, Ashworth A, Hall A. 1995. An essential role for Rho, Rac, and Cdc42 GTPases in cell cycle progression through G1. Science 269:1270–1272.

Peitsch M, Polzar B, Stephan H, et al. 1993. Characterization of the endogenous deoxyribonuclease involved in nuclear DNA degradation during apoptosis (programmed cell death). EMBO J 12:371–377.

Pollard T, Cooper J. 1986. Actin and actin binding proteins: a critical evaluation of mechanisms and functions. Annu Rev Biochem 55:987–1035.

Prasad G, Fuldner R, Cooper H. 1993. Expression of transduced tropomyosin 1 cDNA suppresses neoplastic growth of cells transformed by the *ras* oncogene. Proc Natl Acad Sci USA 90:7039–7043.

Rao J, Bonner R, Hurst R, Reznikoff C, Hemstreet G. 1997. Quantitative changes in cytoskeletal and nuclear actins during cellular transformation. Int J Cancer 70:423–429.

Rauch F, Polzar B, Stephan H, et al. 1997. Androgen ablation leads to an upregulation and intranuclear accumulation of deoxyribonuclease I in rat prostate epithelial cells paralleling their apoptotic elimination. J Cell Biol 137: 909–923.

Senderowicz A, Kaur G, Sainz E, et al. 1995. Jas's inhibition of the growth of prostate carcinoma cells in vitro with disruption of the actin cytoskeleton. J Natl Cancer Inst 87:46–51.

Sogin D, Hinkle P. 1980. Binding of cytochalasin B to human erythrocyte glucose transport. Biochemistry 19: 5417–5420.

Tanaka M, Mullauer L, Ogiso Y, et al. 1995. Gelsolin: a candidate for suppressor of human bladder cancer. Cancer Res 55:3228–3232.

Ucker D, Obermiler P, Eckhart W, Apgar J, Berger N, Meyers. 1992. Genome digestion is a dispensable consequence of physiological cell death mediated by cytotoxic T-lymphocytes. Mol Cell Biol 12:3060–3069.

Zhang X, Minale L, Zampella A, Smith C. 1997. Microfilament depletion and circumvention of multiple drug resistance by Sphinxolides. Cancer Res 57:3751–3758.